



Individual and common inhibitors of coronavirus and picornavirus main proteases

Chih-Jung Kuo^{a,b}, Hun-Ge Liu^a, Yueh-Kuei Lo^a, Churl-Min Seong^c, Kee-In Lee^c,
Young-Sik Jung^{c,*}, Po-Huang Liang^{a,b,*}

^aInstitute of Biological Chemistry, Academia Sinica, Taipei 11529, Taiwan, ROC

^bTaiwan International Graduate Program, Academia Sinica, Taipei 11529, Taiwan

^cKorea Research Institute of Chemical Technology, Daejeon 305-606, Republic of Korea

ARTICLE INFO

Article history:

Received 5 November 2008

Revised 17 December 2008

Accepted 23 December 2008

Available online 21 January 2009

Edited by Hans-Dieter Klenk

Keywords:

Coronavirus

Picornavirus

3C protease

Fluorescence assay

High throughput screening

Computer modeling

ABSTRACT

Picornaviruses (PV) and coronaviruses (CoV) are positive-stranded RNA viruses which infect millions of people worldwide each year, resulting in a wide range of clinical outcomes. As reported in this study, using high throughput screening against ~6800 small molecules, we have identified several novel inhibitors of SARS-CoV 3CL^{pro} with IC₅₀ of low μM. Interestingly, one of them equally inhibited both 3C^{pro} and 3CL^{pro} from PV and CoV, respectively. Using computer modeling, the structural features of these compounds as individual and common protease inhibitors were elucidated to enhance our knowledge for developing anti-viral agents against PV and CoV.

© 2009 Federation of European Biochemical Societies. Published by Elsevier B.V. All rights reserved.

1. Introduction

Picornaviruses (PV) are small nonenveloped RNA viruses with a single strand of genomic RNA of 7500–8000 nucleotides [1]. The members of PV include rhinoviruses (RV), enteroviruses (EV), coxsackieviruses (CV), polioviruses, echoviruses, encephalomyocarditis viruses, meningitis virus, foot and mouth viruses, hepatitis A virus, and so on. Among them, RV is the major cause of the common cold, whereas EV and CV infection can cause hand, foot, and mouth diseases in human and animals. In severe cases, EV can damage the central nervous systems leading to viral meningitis, encephalitis, and severe myocarditis, as well as fatal pulmonary edema [2–5]. CV strain B is a major human pathogen that causes meningitis and myocarditis leading to heart failure in young adults and congestive heart failure [6]. In these PV, a chymotrypsin-like protease (named 3C^{pro}) is required to process polyproteins into mature proteins for viral replication, which represents a promising anti-viral drug target [7].

On the other hand, coronaviruses (CoV) are the positive-stranded RNA viruses with larger genome of 27–32 kb, which typically cause respiratory and enteric diseases, pneumonia, exacerbation of asthma, neurological symptoms, and myocarditis in humans and domestic animals. An outbreak of severe acute respiratory syndrome (SARS), caused by a novel human CoV, was spread from China to 29 countries in 2003, infecting a total of ~8000 people and killing ~800 patients [8]. SARS-CoV contains a 3C-like protease (3CL^{pro}) analogous to the 3C^{pro} of PV, responsible for processing two overlapping polyproteins, pp1a (486 kDa) and pp1ab (790 kDa). Other members of human CoV including CoV-229E, CoV-OC43, CoV-HKU1, and CoV-NL63 also require a 3CL^{pro} in the maturation of viral proteins.

Several inhibitors have been developed to inhibit the 3C^{pro} of RV and EV [9–12] and 3CL^{pro} of SARS-CoV [13–15]. However, their inhibitors can not be mutually used without modification. For example, AG7088, a potent inhibitor of RV and other picornaviral 3C^{pro} [16], failed to inhibit SARS-CoV 3CL^{pro} [17]. Unlike the 3CL^{pro}, which is dimeric and in which each subunit is composed of three domains, the 3C^{pro} is a monomer with only the two catalytic domains. The structure-based sequence alignment (Fig. 1) shows some sequence differences, which may alter inhibitor specificity. In this study, we performed high throughput screening using a library of ~6800 compounds to find five novel inhibitors of the

* Corresponding authors. Address: Institute of Biological Chemistry, Academia Sinica, Taipei 11529, Taiwan, ROC. Fax: +886 2 2788 9759.

E-mail addresses: ysjung@krict.re.kr (Y.-S. Jung), phliang@gate.sinica.edu.tw (P.-H. Liang).

of various concentrations of the inhibitors to obtain the IC_{50} values.

2.4. Computer modeling of the inhibitors binding with the proteases

For the modeling analysis, we used the crystal structure of SARS 3CL^{pro} in complex with a peptide inhibitor (PDB code 1UK4) [19], the structures of CoV-229E 3CL^{pro} and CVB3 3CL^{pro} solved by us, and the structural model of EV71 3CL^{pro} constructed from the structure of RV 3CL^{pro} (PDB code 1CQQ) [20]. Docking process was performed using an automated ligand-docking subprogram of the Discovery Studio Modeling 1.2 SBD (Accelrys Inc., San Diego, CA), with a set of parameters chosen to control the precise operation of the genetic algorithm. Docking runs were carried out using standard default settings “grid resolution” of 5 Å, “site opening” of

12 Å, and “binding site” selected for defining the active site cavity.

3. Results

3.1. Screening of the protease inhibitors

We first screened against a library of ~6800 compounds for inhibiting SARS-CoV 3CL^{pro}. From the primary screening, there were 66 compounds which showed more than 50% inhibition of the enzyme activity at 50 μ M. We further tested their inhibitory activities at 10 μ M and five of them (21155, 22723, 27548, 43146, and 48511) showed IC_{50} values smaller than 10 μ M. According to their dose–response curves as shown in Fig. 2A–E, the five hits 21155, 22723, 27548, 43146, and 48511 displayed

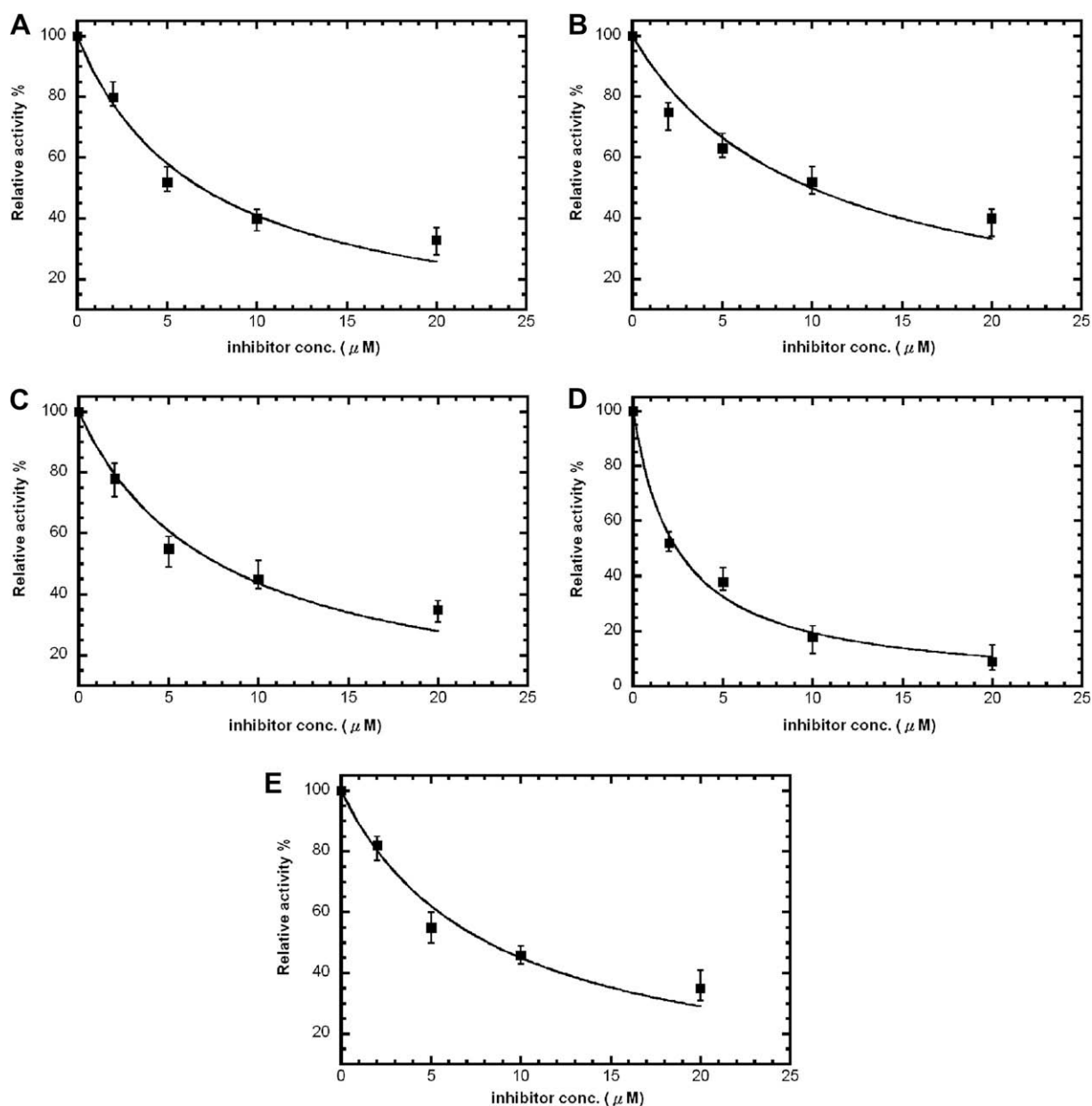
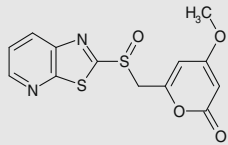
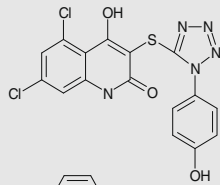
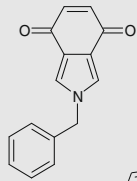
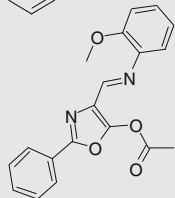
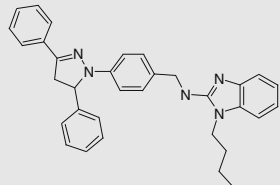


Fig. 2. Dose–response curves for the five hits against SARS-CoV 3CL^{pro} from the screening. IC_{50} values were determined from the curves using equation 1. These were (A) 7.2 ± 0.7 μ M (21155), (B) 10.6 ± 1.3 μ M (22723), (C) 7.0 ± 0.8 μ M (27548), (D) 3.3 ± 0.2 μ M (48511), and (E) 8.1 ± 0.9 μ M (43146). The structures and activities of these inhibitors are summarized in Table 1.

Table 1
Summary of IC₅₀ values (μM) of the five hits with SARS-CoV 3CL^{pro}, and other 3C(L) proteases.

Compound ID	Structure	SARS 3CL	229E 3CL	CVB3 3C	EV71 3C	RV14 3C
21155		7.2 ± 0.7	5.6 ± 1.0	>50	>50	>50
22723		10.6 ± 1.3	12.4 ± 0.8	>50	>50	>50
27548		7.0 ± 0.8	6.6 ± 0.3	>50	>50	>50
48511		3.3 ± 0.2	1.8 ± 0.7	>50	>50	>50
43146		8.1 ± 0.9	10.3 ± 1.1	5.4 ± 0.2	3.3 ± 0.3	5.2 ± 0.6

IC₅₀ values of 7.2 ± 0.7, 10.6 ± 1.3, 7.0 ± 0.8, 3.3 ± 0.2, and 8.1 ± 0.9 μM, respectively, against the SARS 3CL^{pro}. Similar inhibition results were observed for 3CL^{pro} of CoV-229E (data summarized in Table 1), but not for 3C^{pro}. However, 43146 inhibited both 3C^{pro} and 3CL^{pro} with IC₅₀ values of 10.3 ± 1.1 μM, 5.4 ± 0.2 μM, 3.3 ± 0.3, and 5.2 ± 0.6 μM, respectively, against CoV-229E 3CL^{pro}, CVB3 3C^{pro}, EV71 3C^{pro} and RV14 3C^{pro} (Fig. 3A–D and summarized in Table 1). This compound contains a dihydropyrazole ring with three substituents, two phenyl groups and a lengthy N-butyl-benzimidazolylamino-toluene.

3.2. Inhibition potencies of the 43146 analogues

Since 43146 inhibited 3CL^{pro} and 3C^{pro}, its analogues including 45240, 68638, 55688, and 55585 obtained from another compound library were evaluated. As shown in Table 2, all of them showed good potencies against the five proteases. The most potent compound was 45240, and its IC₅₀ values in inhibiting the 3C(L) proteases were measured to be 2.5 ± 0.2 μM (SARS-CoV 3CL^{pro}), 2.6 ± 0.4 μM (CoV-229E 3CL^{pro}), 1.2 ± 0.3 μM (CVB3 3C^{pro}), 0.5 ± 0.1 μM (EV71 3C^{pro}), and 1.7 ± 0.1 μM (RV14 3C^{pro}) (Table 2). This compound contains four rings, three phenyl groups and one imidazole, surrounding a central dihydropyrazole ring, without the lengthy side chain as seen in 43146. Compound 68638 with benzylcyclohexane ring fused with the dihydropyrazole ring and acetyl and iodobenzyl groups attached to the central ring showed less inhibition against both 3C^{pro} and 3CL^{pro} (Table 2). The other two compounds, 55688 and 55585, with shorter side chains attached

to the benzimidazolyl group showed similar inhibitory activities as compared to 43146 (Table 2).

3.3. Computer modeling of 21155, 22723, 27548, and 48511 binding to the proteases

These inhibitors are competitive inhibitors with respect to the substrate (data not shown), indicating they bind in the active site. To rationalize the binding discrepancy of these inhibitors against these proteases, their binding modes with SARS-CoV 3CL^{pro} and four other proteases were modeled and some of them are shown in Fig. 4. The first four inhibitors of SARS-CoV 3CL^{pro} are more rigid because the thiazolopyridine in 21155, the dichlorobenzoquinoline in 22723, the isindole-1,3-dione in 27548, and the oxazole in 48511 adopt planar structures and the three substituents of the oxazole ring in 48511 are fixed in a conformer, due to the 1,2-steric interaction between the acetate group and the N-aryl imino group as well as the biaryl interaction between the phenyl and oxazole to prohibit their free rotation. All these compounds can be considered as two rigid aromatic moieties connected by a small linker. Based on the computer modeling, each of these aromatic moieties is bound to S1 or S2 site of SARS protease by forming H-bonds and hydrophobic interactions (Fig. 4A–D). As shown in the computer modeling, Glu166 side chain of SARS 3CL^{pro} forms H-bonds with these four inhibitors. However, the corresponding amino acid residue in 3C^{pro} is Gly164, which lacks the side chain to form H-bond with any of these compounds (also see Fig. 4F), leading to loss of inhibition. In addition, the 3C^{pro} have more open but shallow S2

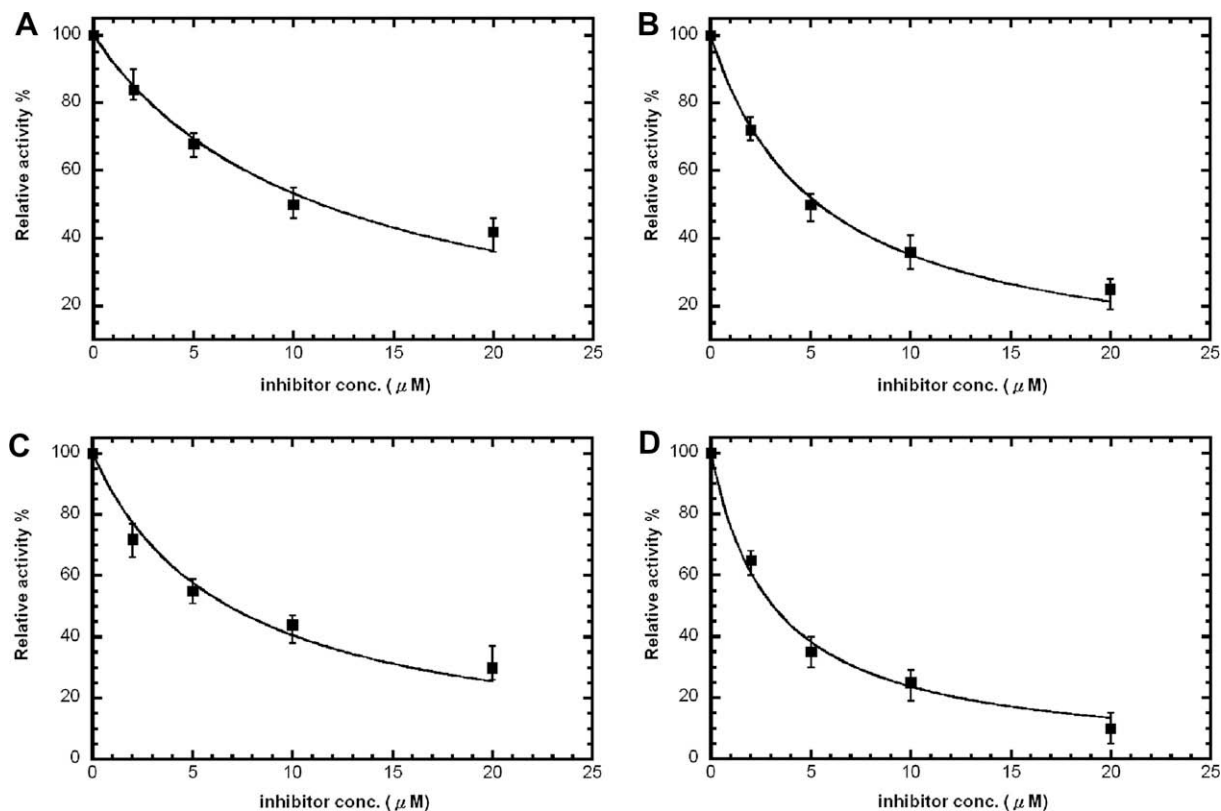


Fig. 3. Dose–response curves for 43146 against 229E 3CL^{PRO}, CVB3 3C^{PRO}, EV71 3C^{PRO} and RV14 3C^{PRO}. IC₅₀ values were determined from the curves using equation 1. These were (A) 10.3 ± 1.1 μM (229E 3CL^{PRO}), (B) 5.4 ± 0.2 μM (CVB3 3C^{PRO}), (C) 3.3 ± 0.3 μM (EV71 3C^{PRO}), and (D) 5.2 ± 0.6 μM (RV14 3C^{PRO}).

Table 2

IC₅₀ values (μM) of compound 43146 analogs with SARS-CoV 3CL^{PRO}, and other 3C(L) proteases.

Compound ID	Structure	SARS 3CL	229E 3CL	CVB3 3C	EV71 3C	RV14 3C
45240		2.5 ± 0.2	2.6 ± 0.4	1.2 ± 0.3	0.5 ± 0.1	1.7 ± 0.1
68638		9.8 ± 0.8	12.4 ± 0.8	7.0 ± 0.8	10.6 ± 1.3	5.3 ± 1.1
55688		8.0 ± 0.5	9.6 ± 0.3	6.1 ± 0.5	8.5 ± 0.6	7.7 ± 1.0
55585		8.4 ± 0.2	10.2 ± 0.7	6.5 ± 0.6	4.7 ± 0.2	6.4 ± 0.3

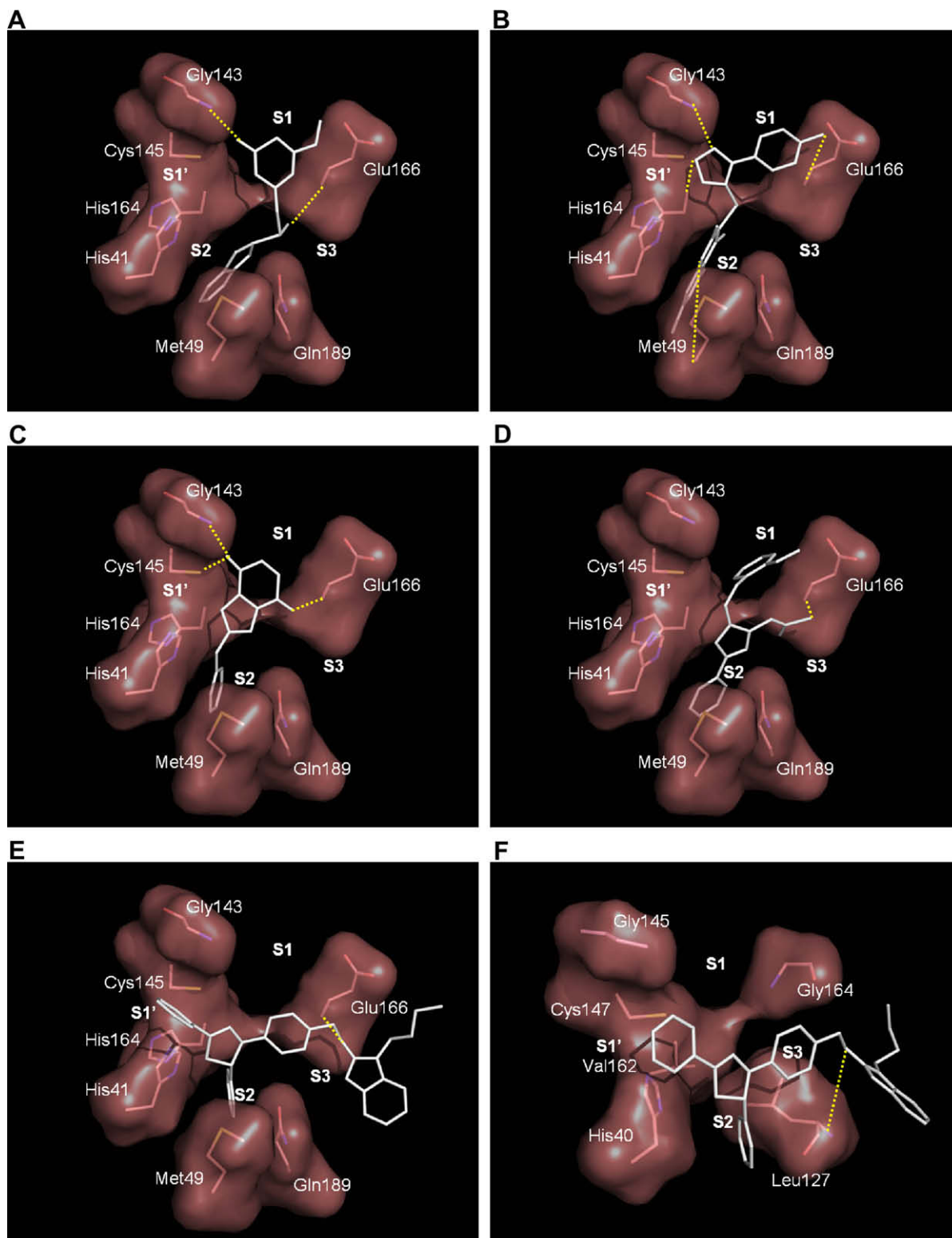


Fig. 4. Computer modeling of the binding modes of the inhibitors in the active site of the SARS 3CL^{Pro}. The more rigid moieties of the inhibitors 21155, 22723, 27548, 48511 are probably bound to S1 and S2 sites as shown in (A), (B), (C), and (D), respectively. (E) 43146 binds SARS-CoV 3CL^{Pro} differently with the biphenyl 4,5-dihydro-1H-pyrazole moiety anchored at the S1' and S2 sites and the rest of the molecule at the S3 and the following sites. The hydrogen bond interactions were represented by yellow dotted lines.

site (due to its partial blockage by Leu127) than 3CL^{Pro} according to the crystal structures of RV 3C^{Pro} [20] and CVB3 3C^{Pro} (Lee et al., unpublished results) compared to 3CL^{Pro} (also see Fig. 4F). Thus, 3C^{Pro} can not hold these compounds tightly.

3.4. Binding modes of 43146 and its analogues to the proteases

In contrast, the compound 43146 is more flexible, because the dihydropyrazole is not planar, and the phenyl group is linked to

the sp³-hybridized carbon of the dihydropyrazole ring, so it is free for rotation. Different from the binding modes of the other 4 inhibitors, the diphenyl 4,5-dihydro-1H-pyrazole moiety of 43146 fits well at the S1' and S2 sites in the SARS 3CL^{pro} (Fig. 4E) with the rest of the molecule at the S3 site and beyond. With this binding mode, the compound was predicted to also bind well in the 3C^{pro}, consistent with the inhibition data. In fact, RV 3C^{pro} prefers a phenyl group at the S2 site as evidenced by its strong inhibition by AG7088 which has a P2-fluorophenylalanine. Thus, it could be rationalized by computer modeling that only 43146 among the five hits can inhibit the three 3C^{pro} in addition to the 3CL^{pro}.

The analogues of 43146, including 45240, 68638, 55688, and 55585, bind in the 3C^{pro} and 3CL^{pro} active sites with similar modes to that of 43146 (data not shown). Compared to 43146, 55688 and 55585 only have minor structural difference with shorter alkyl groups attached to the benzimidazole ring, so that they showed similar inhibition against the proteases. The fused ring system and the phenyl group in 68638 may also span from S1' to S2 sites in both kinds of proteases, yielding similar inhibition. However, 45240 showed a significantly better inhibition against the 3C^{pro} than 43146. Apparently, the lengthy side chain attached to the phenyl group in the compound did not provide additional interaction with the protease, consistent with the binding mode shown in Fig. 4E. However, the additional interaction is provided by the pyridine ring bound near the more open S1' site in 3C^{pro}.

4. Discussion

AG7088 is the best inhibitor identified so far for 3C^{pro}, which not only inhibits the 3C^{pro} from RV, but also those from CV and EV [16]. However, it did not inhibit 3CL^{pro} from SARS-CoV [17]. This may be partially due to the blockage of its P1-lactam ring by the relatively larger Glu166 side chain and also the S2 site of 3CL^{pro} is narrower although it is deeper. Therefore, when the P2-phenylalanine is changed to non-planar leucine or cyclohexane without changing the P1-lactam, they became good inhibitors of SARS 3CL^{pro} [21]. Unlike AG7088, which is a ketomethyl isostere of a tripeptide-conjugated ester, compound 43146 is not peptide-like. From the random screening as shown in the study, we have found a starting point toward the development of non-peptide multiple-function inhibitors against CoV and PV. With further modification of these individual and common inhibitors of the viral proteases, we hope to find solution for the possible reoccurrence of SARS and other diseases caused by the viruses with the 3C^{pro} and 3CL^{pro}.

Acknowledgements

This work was supported by a grant from Academia Sinica to PHL, and we thank Korea Chemical Bank for providing their chemical library with which this work was conducted.

References

- [1] Melnick, J.L. (1996) Enterovirus: polioviruses, coxsackieviruses, echoviruses, and newer enteroviruses. In *Virology*, 3rd ed., Lippincott-Raven, Philadelphia, PA.
- [2] Blomberg, K. et al. (1974) New enterovirus type associated with epidemic of aseptic meningitis and/or hand, foot, and mouse disease. *Lancet* 2, 112.
- [3] Sperber, S.J. and Hayden, F.G. (1998) Chemotherapy of rhinovirus colds. *Antimicrob. Agents Chemother.* 32, 409–414.
- [4] Lum, L.C. et al. (1998) Neurogenic pulmonary oedema and enterovirus 71 encephalomyelitis. *Lancet* 352, 1391.
- [5] Ho, M. et al. (1999) An epidemic of enterovirus 71 infection in Taiwan. Taiwan Enterovirus Epidemic Working Group. *New Engl. J. Med.* 341, 929–935.
- [6] Lee, C.K. et al. (2005) Characterization of an infectious cDNA copy of the genome of a naturally occurring, avirulent coxsackievirus B3 clinical isolate. *J. Gen. Virol.* 86, 197–210.
- [7] Krausslich, H.G. and Wimmer, E. (1998) Viral proteinases. *Annu. Rev. Biochem.* 57, 701–754.
- [8] Ksiazek, T.G. et al. (2003) A novel coronavirus associated with severe acute respiratory syndrome. *New Eng. J. Med.* 348, 1953–1966.
- [9] Patick, A.K. (2006) Rhinovirus chemotherapy. *Antiviral Res.* 71, 391–396.
- [10] Lee, E.S. et al. (2007) Development of potent inhibitors of the coxsackievirus 3C protease. *Biochem. Biophys. Res. Commun.* 358, 7–11.
- [11] Maugeri, C. et al. (2008) New anti-viral drugs for the treatment of the common cold. *Bioorg. Med. Chem.* 16, 3091–3107.
- [12] Kuo, C.J. et al. (2008) Design, synthesis, and evaluation of 3C protease inhibitors as anti-enterovirus 71 agents. *Bioorg. Med. Chem.* 16, 7388–7398.
- [13] Liang, P.H. (2006) Characterization and inhibition of SARS-coronavirus main protease. *Curr. Top Med. Chem.* 6, 361–376.
- [14] De Clercq, E. (2006) Potential antivirals and antiviral strategies against SARS coronavirus infections. *Expert Rev. Anti Infect. Ther.* 4, 291–302.
- [15] Zhai, S., Liu, W. and Yan, B. (2007) Recent patents on treatment of severe acute respiratory syndrome (SARS). *Recent Patents Anti-Infect Drug Disc.* 2, 1–10.
- [16] Binford, S.L. et al. (2005) Conservation of amino acids in rhinovirus 3C protease correlates with broad-spectrum activity of rupintrivir, a novel rhinovirus 3C protease inhibitor. *Antimicrob. Agents Chemother.* 49, 619–626.
- [17] Shie, J.J. et al. (2005) Inhibition of the severe acute respiratory syndrome 3CL protease by peptidomimetic α,β -unsaturated esters. *Bioorg. Med. Chem.* 13, 5240–5252.
- [18] Kuo, C.J. et al. (2004) Characterization of SARS main protease and inhibitor assay using a fluorogenic substrate. *Biophys. Biochem. Res. Commun.* 318, 862–867.
- [19] Yang, H. et al. (2003) The crystal structures of severe acute respiratory syndrome virus main protease and its complex with an inhibitor. *Proc. Natl. Acad. Sci. USA* 100, 13190–13195.
- [20] Matthews, D.A. et al. (1999) Structure-assisted design of mechanism-based irreversible inhibitors of human rhinovirus 3C protease with potent antiviral activity against multiple rhinovirus serotypes. *Proc. Natl. Acad. Sci. USA* 96, 11000–11007.
- [21] Yang, S. et al. (2007) Synthesis, crystal structure, structure-activity relationships, and antiviral activity of a potent SARS coronavirus 3CL protease inhibitor. *J. Med. Chem.* 49, 4971–4980.